

Novel Nanoparticles Formed via Self-Assembly of Poly(ethylene glycol-*b*-sebacic anhydride) and Their Degradation in Water

Chi Wu,^{*,†,‡} Jie Fu,^{‡,§} and Yue Zhao[†]

The Open Laboratory of Bond-selective Chemistry, Department of Chemical Physics, University of Science and Technology of China, Hefei, Anhui, China; Department of Chemistry, The Chinese University of Hong Kong, Shatin, N.T., Hong Kong; and College of Material Science and Engineering, Wuhan University of Technology, Wuhan, Hubei, China

Received June 6, 2000; Revised Manuscript Received September 19, 2000

ABSTRACT: A novel diblock copolymer, poly(ethylene oxide-*b*-sebacic acid) (PEO-*b*-PSA), was prepared by polycondensation. Its self-assembly in water via a microphase inversion resulted in narrowly distributed stable polymeric nanoparticles with a size of ~70 nm. Such formed nanoparticles had a core-shell nanostructure with the insoluble hydrophobic PSA blocks as the core and the soluble hydrophilic PEO blocks as the protective shell. The core was degradable, and its degradation led to the disintegration of the nanoparticle. The structure of the nanostructure and the degradation kinetics were investigated by a combination of static and dynamic laser light scattering. Our results indicated that the degradation was a first-order reaction, and the degradation rate increases with the dispersion temperature.

Introduction

The potential use of polymeric particles as drug carriers has attracted much attention, because drugs can be released in a controllable fashion and the particle size can be regulated to target different organs.^{1–10} Moreover, these particles can be made in different dosage forms, including intravenous and oral routs, to increase drug's bioavailability and reduce some associated adverse effects. It was shown that a decrease of the particle size could reduce the irritant reaction at the injection site.¹¹ Narrowly distributed polymeric nanoparticles in the size range 10–100 nm are ideal for intravenous injection, and they can easily pass through the narrowest blood capillary with a diameter of ~4 μm .¹²

It is nature to seek a biodegradable and biocompatible polymer as a drug carrier because its absorption by body can avoid the removing, often surgically, of an implanted drug releasing device.^{13–17} Polyanhydride as a biodegradable polymer has been widely used due to its biocompatibility.^{18–23} Previously, we have shown that surfactant could be used to prepare polysebacic anhydride (PSA) nanoparticles stable in aqueous solution. However, the nanoparticles stabilized by surfactant molecules are sensitive to the ionic strength and pH, which are not suitable for some biomedical applications.

On the other hand, extensive fundamental studies have shown that block and graft copolymers could form polymeric micelles via a self-assembly in selective solvents.^{24–27} In biomedical applications, poly(ethylene glycol)-coated nanoparticles have attracted a particular attention since PEG is nontoxic and has a low protein adsorption and cell adhesion.^{28,29} The most important is that the internal use of PEG in the human body has been approved by the Food and Drug Administration (FDA).³⁰ In this study, we combined polyanhydride and

poly(ethylene glycol) into a novel biocompatible and biodegradable diblock copolymer, poly(ethylene oxide-*b*-sebacic acid) (PEO-*b*-PSA), and successfully micronized this water-insoluble polymer into polymeric nanoparticles stable in water via a microphase inversion. The structure and degradation of such formed PEO-*b*-PSA nanoparticles were investigated by a combination of static and dynamic laser light scattering (LLS).

Experimental Section

Sample Preparation. Poly(ethylene glycol) methyl ether ($M_n = 5000$ and $M_w/M_n \sim 1.3$) was vacuum-dried. Sebacic acid was recrystallized three times from ethanol. Acetic anhydride was purified by distillation. Tetrahydrofuran (THF) and chloroform were refluxed and distilled over calcium hydride. Toluene and *n*-hexane were predried over 4 Å molecular sieves and distilled. Ethyl ether was refluxed and distilled over sodium wire. Other reagents were used as received without further purification. Poly(ethylene oxide-*b*-sebacic acid) (PEO-*b*-PSA) was synthesized by melt polycondensation of sebacic acid and poly(ethylene glycol) methyl ether. The synthesis is outlined as follows.

Refluxing of sebacic acid in acetic anhydrides resulted in a mixture of anhydride oligmers. The resultant oligmers were recrystallized from toluene and washed with *n*-hexane. The polymerization of these oligmers and poly(ethylene glycol) methyl ether was conducted in a glass tube ~35 cm^3 with a nitrogen inlet at 180 °C under 0.01 mmHg. Note that the PEO macromonomer has only one reacting end group. The resultant low molar mass was collected under vacuum in a liquid nitrogen trap. The resultant diblock copolymer was purified by precipitation in dry ether from chloroform solution and washed with cold water. The average molar mass of poly(ethylene oxide-*b*-sebacic acid) used in this study was 2.52×10^4 g/mol, and the polydispersity index is less than 1.5. The compositions of poly(ethylene oxide-*b*-sebacic acid) were estimated by ¹H NMR and FT-IR. The NMR spectra were recorded in CDCl₃ on a Bruker DPX-300 (300 MHz) spectrometer, while the FT-IR spectra were recorded on a Nicolet Impact 420FT-IR spectrometer.

The self-assembly of poly(ethylene oxide-*b*-sebacic acid) was induced by adding a 1 mL solution of PEO-*b*-PSA in THF dropwise into 99 mL of deionized water under ultrasonification. As expected, THF quickly mixed with water. The water-insoluble PSA blocks collapsed and aggregated to form a core,

[†] University of Science and Technology of China.

[‡] The Chinese University of Hong Kong.

[§] Wuhan University of Technology.

* To whom correspondence should be addressed. Tel +852-2609-6106; Fax +852-2603-5057; E-mail chiwu@cuhk.edu.hk.

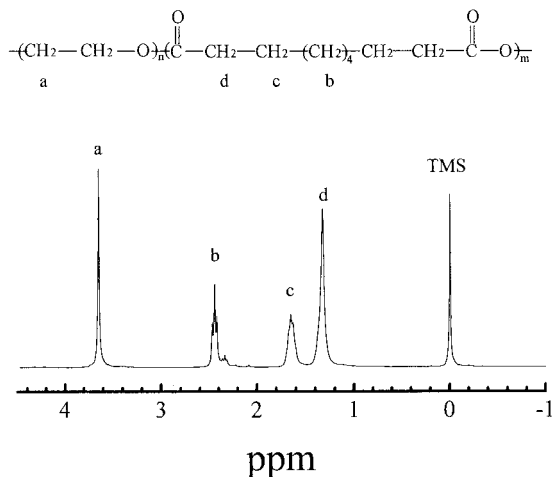


Figure 1. Typical ^1H NMR spectrum of poly(ethylene oxide-*b*-sebacic acid) in CDCl_3 .

while the water-soluble PEO blocks formed a protective shell. Such formed nanoparticles were stable in water over months. The small amount (1%) of THF introduced in the preparation was removed under a reduced pressure, which had no effect on the particle size and stability. The pH of the dispersion was adjusted by NaOH. In a typical degradation experiment, a proper amount of the dust-free NaOH aqueous solution was in situ added into a 2 mL dust-free dispersion.

Laser Light Scattering (LLS). A modified commercial LLS spectrometer (ALV/SP-125) equipped with an ALV-5000 multi- τ digital time correlator and a solid-state laser (DPSS, out power = ~ 400 mW at $\lambda = 532$ nm) was used. In static LLS, the angular dependence of the excess absolute time-average scattered intensity, i.e., Rayleigh ratio $R_v(q)$, of a dilute dispersion can lead to the weight-average molar mass M_w , the second virial coefficient A_2 , and the root-mean-square z -average radius $\langle R_g^2 \rangle_z^{1/2}$ (or simply as $\langle R_g \rangle$),³¹ where q is the scattering vector. In dynamic LLS, the Laplace inversion of a measured intensity-intensity-time correlation function $G^{(2)}(t, q)$ in the self-beating mode results in a line-width distribution $G(\Gamma)$.^{31,32} For a pure diffusive relaxation, $(\Gamma/q^2)_{q \rightarrow 0, c \rightarrow 0}$ leads to the translational diffusion coefficient D or further to the hydrodynamic radius R_h via the Stokes-Einstein equation. Both $R_v(q)$ and $G^{(2)}(t, q)$ were simultaneously measured during the degradation. The detail of LLS theory can be found elsewhere.^{31,32} Both the PEO-*b*-PSA nanoparticle dispersion and NaOH aqueous solution used in LLS were clarified respectively by 0.8 and 0.1 μm Millipore filters to remove dust.

Results and Discussion

Figure 1 shows a typical ^1H NMR spectrum of the PEO-*b*-PSA block copolymer. The peak at 3.65 ppm is a typical NMR signal for the methylene protons on PEO, indicating that PEO was successfully copolymerized with PSA. The peaks at 2.44, 1.65, and 1.32 ppm are attributed to the methyl protons of PSA. By taking the area ratio of the methylene protons of PEO to that of PSA, we estimated weight percentage of PEO (wt %) in the copolymer to be 19.7%, and the copolymer has an average molar mass of 2.54×10^4 g/mol. The typical IR anhydride double peak of PEO-*b*-SA was appeared at 1809 and 1741 cm^{-1} .

Figure 2 shows a typical Berry plot of the PEO-*b*-PSA nanoparticles in water at 25 $^\circ\text{C}$, which incorporates the angular and concentration dependence of Rayleigh ratio $R_v(q)$ on a single grid. The extrapolation of $[KC/R_{vV}(q)]^{1/2}$ to $C \rightarrow 0$ and $q \rightarrow 0$ leads to M_w . The slopes of $[KC/R_{vV}(q)]^{1/2}_{C \rightarrow 0}$ vs q^2 and $[KC/R_{vV}(q)]^{1/2}_{q \rightarrow 0}$ vs C respectively lead to $\langle R_g \rangle$ and A_2 . Figure 3 shows a typical dynamic LLS result, which reveals that the nanopar-

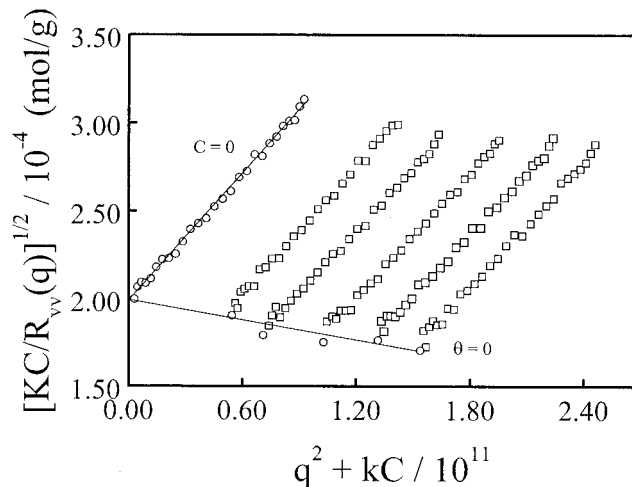


Figure 2. Typical Zimm plot of PEO-*b*-PSA nanoparticles in aqueous solution at 25 $^\circ\text{C}$, where C ranges from 4.05×10^{-6} to 1.14×10^{-5} g/mL, K is a constant for a given solution and temperature, and k is a constant to spread the plot.

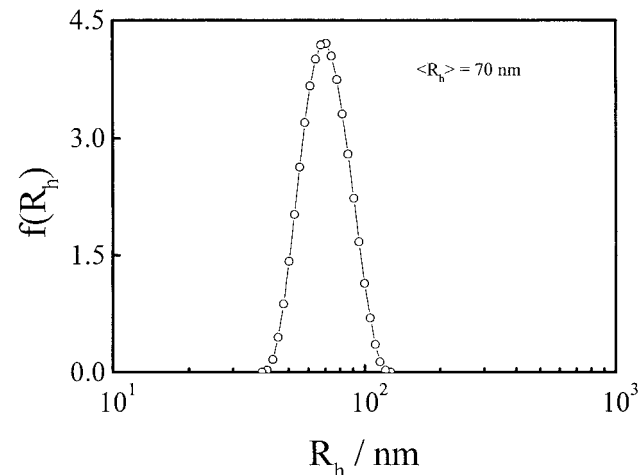


Figure 3. Typical hydrodynamic radius distribution $f(R_h)$ of PEO-*b*-PSA nanoparticles in aqueous solution at 25 $^\circ\text{C}$, where $C = 1.14 \times 10^{-5}$ g/mL.

Table 1. Static and Dynamic Laser Light Scattering Characterization of PEO-*b*-PSA Nanoparticles in Water at 25 $^\circ\text{C}$ ^a

$M_{w, \text{particle}}$ (g/mol)	A_2 (mol cm^3/g^2)	$\langle R_h \rangle$ (nm)	$\langle R_g \rangle / \langle R_h \rangle$	$N_{\text{aggregation}}$	$\langle \rho \rangle$ (g/cm^3)
2.6×10^7	-3.0×10^{-4}	70	1.0	1.1×10^3	3.1×10^{-2}

^a Relative error: M_w , $\pm 5\%$; $\langle R_g \rangle$, $\pm 8\%$; and $\langle R_h \rangle$, $\pm 2\%$.

ticles in water at 25 $^\circ\text{C}$ are very narrowly distributed with an average hydrodynamic radius $\langle R_h \rangle$ of ~ 70 nm, calculated from $f(R_h)$ by $\int_0^\infty f(R_h) R_h dR_h$.

Table 1 summarizes all light scattering results for the PEO-*b*-PSA nanoparticles in water, where the average number (N_{agg}) of the copolymer chains inside each particle and the average particle density $\langle \rho \rangle$ were estimated from $M_{w, \text{particle}}$, $M_{w, \text{chain}}$, and $\langle R_h \rangle$. The ratio of $\langle R_g \rangle / \langle R_h \rangle \sim 1.0$ is slightly higher than 0.774 predicted for a uniform nondraining sphere, indicating that such formed nanoparticles are partially draining, because of the hydrophilic PEO blocks.³³ The fact that $\langle \rho \rangle$ is much lower than ~ 1.0 g/cm³ expected for a bulk polymer also indicates that the nanoparticle contains loosely aggregated chains and contains a lot of water in its hydrodynamic volume. On average, each PEG chain

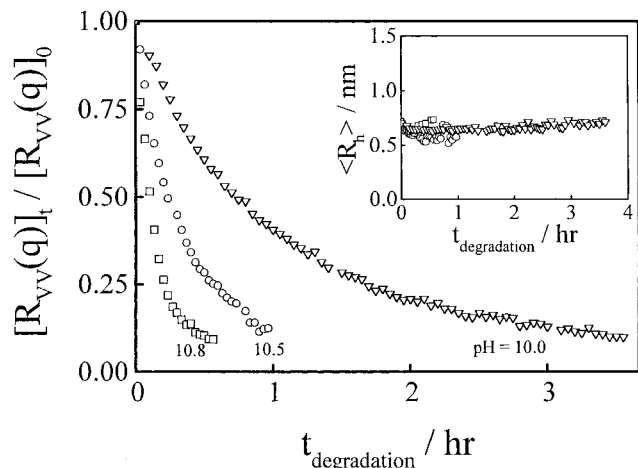


Figure 4. pH dependence of degradation of PEO-*b*-PSA nanoparticles, where C_0 and C_t are the nanoparticle concentrations, respectively, at time 0 and t , $C_0 = 1.14 \times 10^{-5}$ g/mL, and $T = 37^\circ\text{C}$.

occupies a surface area of $\sim 19 \text{ nm}^2$ on the periphery of the nanoparticle, which agrees well with the average size of the PEO blocks in water.

Figure 4 reveals $[R_{vv}(q)]_t/[R_{vv}(q)]_0$ decreases during the degradation. It is known that $R_{vv}(q) \propto CM_w$. In principle, the decrease of $[R_{vv}(q)]_t/[R_{vv}(q)]_0$ can be related to the decrease of either M_w or C or both. However, the inset in Figure 4 shows that there was no change in $\langle R_h \rangle$, i.e., no change in M_w . Apparently, there is a contradiction because the degradation should lead to a decrease in the particle size. The constant particle size actually reveals that the degradation of each particle is so fast that LLS can only "see" the remaining particles during the degradation, not those degraded products with a lower molar mass, because the scattered light intensity is proportional to the square of molar mass. Therefore, the decrease of $[R_{vv}(q)]_t/[R_{vv}(q)]_0$ actually reflects the decrease in the number of the nanoparticles, i.e., the decrease of the relative concentration (C/C_0). A combination of static and dynamic LLS results reveals that the degradation of these nanoparticles are not simultaneous, but in a one-by-one fashion.

The data can be well fitted by $[R_{vv}(q)]_t/[R_{vv}(q)]_0 = e^{-kt}$, indicating that degradation follows a first-order kinetics. It is clear that pH can greatly affect the degradation rate. Adjusting pH, we can control the degradation from a few hours to a few days or even longer. Figure 5 indicates that of the degradation is also influenced by temperature. The degradation rate increases with the temperature. The least-squares fitting of each set of " C/C_0 versus t " leads to degradation rate constant k . The inset shows a typical Arrhenius plot for the degradation, i.e., $k \propto e^{-E_a/RT}$. On the basis of this plot, we were able to estimate the activation energy (E_a) of the degradation to be 44 kJ/mol.

In summary, a novel poly(ethylene oxide-*b*-sebacic acid) (PEO-*b*-PSA) diblock polymer has been synthesized. The self-assembly of this water-insoluble diblock copolymer can lead to narrowly distributed nanoparticles stable in water via a microphase inversion. The PEO-*b*-PSA nanoparticles have a core-shell structure with the core and the shell respectively made of the insoluble/degradable PSA blocks and the PEG blocks. The degradation of the core leads to the dissolution of the nanoparticles. The degradation of each PEO-*b*-PSA nanoparticle is too fast to be observed in laser light

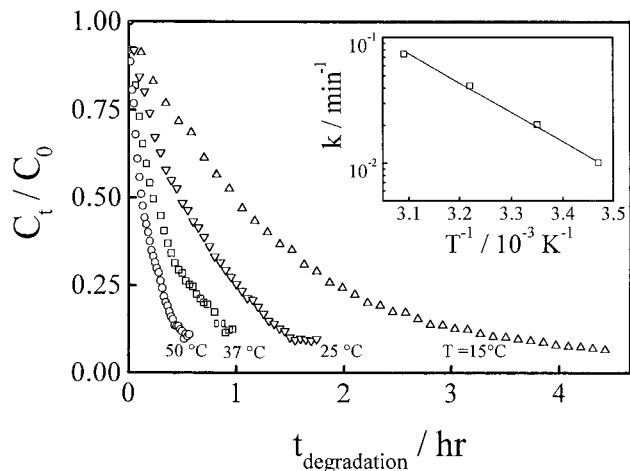


Figure 5. Temperature dependence of degradation of PEO-*b*-PSA nanoparticles, where C_0 and C_t are the nanoparticle concentrations respectively at time 0 and t , $C_0 = 1.14 \times 10^{-5}$ g/mL, and pH = 10.5.

scattering. Our results reveal that the degradation follows a first-order kinetics, and the degradation rate can be regulated by pH and temperature. The activation energy of the degradation is 44 kJ/mol. This study provides a foundation for further biomedical applications of this novel copolymer.

Acknowledgment. The financial support of the National Distinguished Young Investigator Fund (1996, A/C No. 29625410), the National Natural Science Foundation (29974027), and the Research Grants Council of Hong Kong Special Administration Region Earmarked Grant 1998/99 (CUHK 4209/99P, 2160122) is gratefully acknowledged.

References and Notes

- (1) Kreuter, J. M. In *Microcapsules and Nanoparticles in Medicine and Pharmacy*; Donbrow, M., Ed.; CRC Press: Boca Raton, FL, 1992; pp 126–143.
- (2) Sanchez, A.; Vila-Jato, J. L.; Alonso, M. J. *Int. J. Pharm.* **1993**, *99*, 263.
- (3) Fessi, H.; Puisieux, F.; Devissaguet, J. P.; Benita, S. *Int. J. Pharm.* **1989**, *55*, R1.
- (4) Gaspar, R.; Opperdoes, F. R.; Preat, V.; Roland, M. *Ann. Trop. Med. Parasitol.* **1992**, *86*, 41.
- (5) Fallouh, N.; Roblot-Treupel, L.; Fessi, H.; Devissaguet, J. P.; Puisieux, F. *Int. J. Pharm.* **1986**, *28*, 125.
- (6) Dange, C.; Michel, C.; Aprahamian, M.; Couvreur, P. *Diabetes* **1988**, *37*, 246.
- (7) Lemoine, D.; Francois, C.; Kedzierwicz, F.; Preat, V.; Hoffman, M.; Maincent, P. *Biomaterials* **1996**, *17*, 2191.
- (8) Gan, Z.; Jim, T. F.; Li, M.; Zhao, Y.; Wang, S. G.; Wu, C. *Macromolecules* **1999**, *32*, 590.
- (9) Chiannikulchai, N.; Driouich, Z.; Benoit, J. P. *Select. Cancer Therapeut.* **1989**, *5*, 1.
- (10) Fattal, E.; Youssef, M.; Couvreur, P.; Andremont, A. *Antimicrob. Agents Chemother.* **1989**, *33*, 1540.
- (11) Little, K.; Parkhouse, J. *Lancet* **1962**, *2*, 857.
- (12) Thews, G.; Mutschler, E.; Vaupel, P. *Anatomie, Physiologie, Pathophysiologie des Menschen*; Wissenschaftl. Verlagsges.: Stuttgart, 1980; p 229.
- (13) Peppas, N.; Langer, R. *Science* **1994**, *263*, 1715.
- (14) Langer, R. *Science* **1990**, *249*, 1527.
- (15) Langer, R.; Vacanti, J. *Science* **1993**, *260*, 920.
- (16) Song, C. X.; Labhasetwar, V.; Murphy, H.; Qu, X.; Humphrey, W. R.; Shebuski, R. J.; Levy, R. J. *J. Controlled Release* **1997**, *43*, 197.
- (17) Sah, H. K.; Toddywala, R.; Chien, Y. W. *J. Controlled Release* **1994**, *30*, 201.
- (18) Mathiowitz, E.; Amato, C.; Dor, P.; Langer, R. *Polymer* **1990**, *31*, 547.

- (19) Mathiowitz, E.; Saltzman, W.; Domb, A.; Dor, P.; Langer, R. *J. Appl. Polym. Sci.* **1988**, *35*, 755.
- (20) Gao, J.; Niklason, L.; Zhao, X.; Langer, R. *J. Pharm. Sci.* **1998**, *87*, 246.
- (21) Ron, E.; Turek, T.; Mathiowitz, E.; Chasin, M.; Hageman, M.; Langer, R. *Proc. Natl. Acad. Sci. U.S.A.* **1993**, *90*, 4167.
- (22) Leong, K. W.; Brott, B. C.; Langer, R. *Polym. Prepr. (Am. Chem. Soc., Div. Polym. Chem.)* **1984**, *25*, 201.
- (23) Brem, H. *Polym. Prepr. (Am. Chem. Soc., Div. Polym. Chem.)* **1990**, *31*, 229.
- (24) Tuzer, Z.; Kratochvil, P. In *Surface and Colloid Science*; Plenum Press: New York, 1993; Vol. 15, pp 1–83.
- (25) Chu, B. *Langmuir* **1995**, *11*, 414.
- (26) Xu, R.; Winnik, M.; Hallett, F. R.; Riess, G.; Croucher, M. D. *Macromolecules* **1991**, *24*, 87.
- (27) Liu, T.; Zhou, Z.; Wu, C.; Chu, B.; Schneider, D. K.; Nace, V. M. *J. Phys. Chem. B* **1997**, *101*, 8808.
- (28) Chiu, H.; Chern, C.; Lee, C.; Chang, H. *Polymer* **1998**, *39*, 1609.
- (29) Sawhney, A.; Pathak, C.; Hubbell, J. *Biomaterials* **1993**, *14*, 1008.
- (30) Harris, J. J. *Macromol. Sci., Rev. Macromol. Chem. Phys.* **1985**, *C25*, 325.
- (31) Chu, B. *Laser Light Scattering*, 2nd ed.; Academic Press: New York, 1991.
- (32) Berne, B.; Pecora, R. *Dynamic Light Scattering*, 2nd ed.; Plenum Press: New York, 1991.
- (33) Wu, C.; Zuo, J.; Chu, B. *Macromolecules* **1989**, *22*, 633.

MA000989+